Nonequilibrium Phase Transitions in a Dual-pumped Silicon Nitride Kerr Optical Parametric Oscillator

Yichen Shen¹, Sashank K. Sridhar¹, Grégory Moille^{2,3}, Fahad A. Shaikh¹, Kartik Srinivasan^{2,3}, Avik Dutt^{1,4,*}

¹Department of Mechanical Engineering, and Institute for Physical Science & Technology (IPST), University of Maryland, College Park, USA.

² Joint Quantum Institute, NIST/University of Maryland, USA.

³ Microsystems and Nanotechnology Division, National Institute of Standards and Technology, USA.

⁴ National Quantum Laboratory at Maryland (QLab), College Park, MD, USA.

^{*} avikdutt@umd.edu

Abstract: We demonstrate spectral phase transitions in dual-pumped Si_3N_4 nanophotonic Kerr optical parametric oscillators with anomalous dispersion. Through pump-power modulation, we observe real-time switching between a near-degenerate signal (0-FSR separation) and non-degenerate signals (4-FSR separation). © 2024 The Author(s)

Optical parametric oscillators (OPO) find myriad applications in nonlinear and quantum optics, from generating squeezed states[1], random numbers[1], and coherent Ising machines[2], to coherent light sources[3] at wavelengths otherwise difficult to access[4–6]. Recently, $\chi^{(3)}$ microresonator-based dual-pumped degenerate OPOs have shown promise in several of these applications[7] especially in the normal dispersion regime[1,8]. On the other hand, nonequilibrium phase transitions have been predicted using both $\chi^{(2)}$ and $\chi^{(3)}$ OPOs[9,10], but their experimental demonstration has been limited to bulk macroscopic $\chi^{(2)}$ OPOs[9] with implications for precision sensing. A $\chi^{(3)}$ -based demonstration of spectral phase transitions would lead to a deeper understanding of the nonlinear dynamics unique to Kerr nonlinear microresonators as opposed to $\chi^{(2)}$ systems, while their on-chip integration would enable compact scalable devices for aforementioned applications in sensing and quantum state generation.

The challenge in observing the predicted spectral phase transitions (Fig. 1(b)) in $\chi^{(3)}$ -microresonators is that thermal nonlinear shifts create a power-dependent dynamical resonator detuning at slow timescales[11,12]. Since the predicted spectral phase transition is dependent on both detuning and pump power, its clear observation needs decoupling of the pump power change from dynamical thermal detuning.

Here we demonstrate real-time spectral phase transitions in a $\chi^{(3)}$ -microresonator by modulating the pump power at timescales (25 µs) faster than the resonator's thermal response time. By using a dual-pumped Si₃N₄ microring with anomalous dispersion (β_2 =-163.8 fs²/mm), we observe sharp transitions between the degenerate regime (whereby the OPO oscillates at the central mode 0) and the non-degenerate regime (where the OPO oscillates at two modes separated by up to four free-spectral ranges (FSRs)). Note that similar fast pump power kicks have been used to access Kerr soliton states in singly-pumped microresonators[11,12]. The 2nd order phase transition is caused by an interplay between nonlinearity and dispersion, which controls the parametric gain curve, as predicted in[9,10].

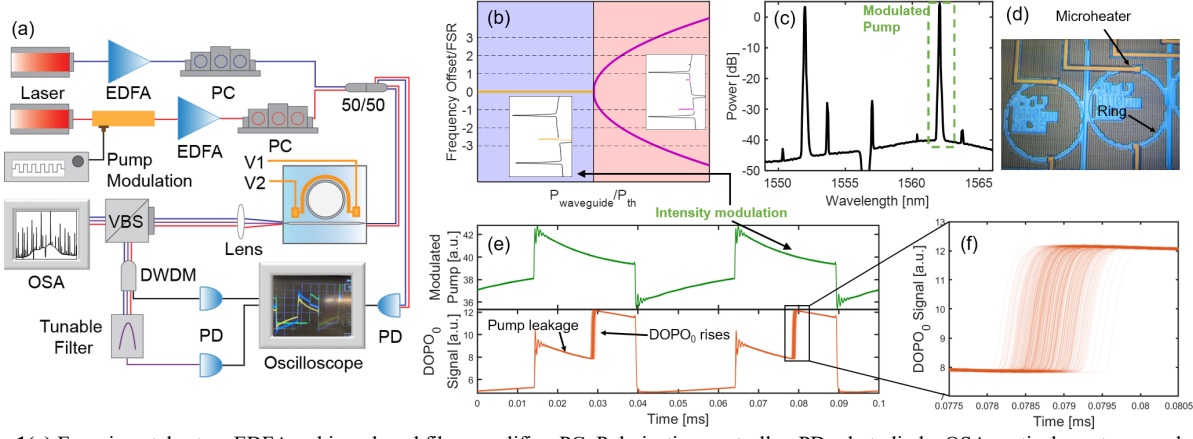


Fig. 1(a) Experimental setup. EDFA: erbium doped fiber amplifier. PC. Polarization controller. PD: photodiode; OSA: optical spectrum analyzer. (b) Phase diagram showing the critical point between degenerate OPO (DOPO, blue region) and non-degenerate OPO (NDOPO, pink region). Insets: Representative OSA spectra measured in each regime with no pump modulation. (c) Measured OSA scan when the intensity modulator is on. The OSA is unable to time-resolve the phase transition and hence both DOPO and nondegenerate signals appear. (d) Microscope image of the device. (e) Superimposed 0.1s-long intensity-modulated pump (@ 20 kHz) and generated DOPO signal. The sharp transition is visible on top of the residual strong pump. (f) Zoomed-in time-resolved view of the DOPO signal, showing the phase transition over 800 runs.

The Kerr OPO is based on a high-Q (Q_i =1.7M) Si_3N_4 microring with a 1.7x0.78 μ m cross section (Fig. 1(d)) and a radius of 110 μ m, corresponding to an FSR of 201 GHz. The OPO is excited by two pumps at 1552.4 nm and 1562.4

nm separated by 6 FSRs, with an on-chip waveguide power of ~40 mW. For monitoring the OPO at slow timescales, we use an OSA. For measurements at fast timescales needed here, we use a tunable filter for the DOPO signal and a channel 27 DWDM filter for the NDOPO signal one FSR away from the degeneracy point (NDOPO₁). A voltage is applied to the microheaters atop the ring to redshift all the resonances to align with the filter bandwidths. Filter outputs are monitored on 75MHz fast photodiodes to simultaneously detect the pump, DOPO and NDOPO signals in a spectro-temporally resolved fashion.

The resonator switches between the DOPO and NDOPO regimes when the 1562 nm pump power is modulated by 40%, and both signals appear on the slow OSA scan (Fig. 1(c)), while without modulation, the DOPO and NDOPO signals appear separately on opposite sides of the critical point depending on the pump power and detuning (Fig. 1(b) insets). The fast photodiode measurements after optical filtering (Fig. 1(e)) show that the NDOPO signals separated by four FSRs rapidly reduces upon reducing the pump power over 25 µs. Thereby, the resonator passes through the critical point and the detected DOPO signal power sharply rises, indicating the spectral phase transition (Fig. 1(f)).

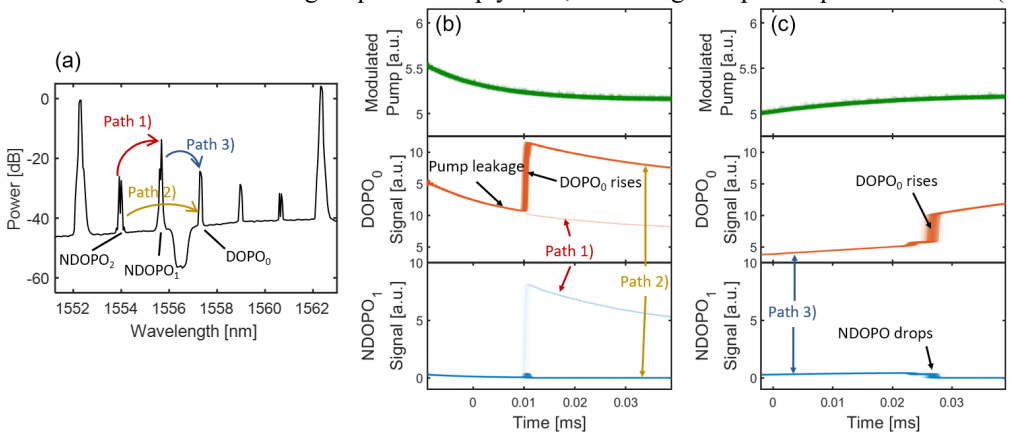


Fig. 2 (a) DOPO signal and two pairs of NDOPO signals, both appearing on a slow OSA scan. (b) 800 superimposed time-resolved scans of DOPO and the NDOPO₁ signals (central and bottom) as the pump power (top) *decreases*. From the intensity of the branches, we deduce two paths: Path 1) the NDOPO₂ signal transitions into the NDOPO₁ signal with a low probability of 5.3%; and Path 2) the NDOPO₂ signal transitions into the DOPO signal. (c) Same as (a) but for *increasing* pump power. Bistability and hysteresis compared to the case of reducing pump power is seen.

Next, we observed that the nonlinear dynamics of Kerr OPOs lead to nondeterministic and bistable switching between DOPO and NDOPO signals with separations of two or four FSRs upon pump power modulation (Fig. 2). Fig. 2(a) shows a scenario when all the resonances in between the two pumps are picked up by the slow scan of OSA, indicating that symmetric pairs of these signals appear at different points along the intensity modulation. Two nondeterministic paths are shown in Fig. 2(b) when the pump power is reduced. For path 1, as the pump power decreases, we observe a sharp increase of NDOPO signal one FSR away from degeneracy (NDOPO₁) while the DOPO signal remains low. The faintness of this path indicates the first path is less likely to happen than path 2, where the DOPO signal sharply rises while the NDOPO signal remains low. This agrees with the phase diagram in Fig. 1(c). However, when the pump power is increased (Fig. 2(c)), we observed that the microring transitions from the NDOPO signal to the DOPO, in contradiction with the phase diagram. This indicates that the bifurcation diagram based on a simple linear stability analysis[9,10] is not sufficient in this complex $\chi^{(3)}$ -based nonlinear system.

We have demonstrated spectral phase transitions in a nanophotonic Si_3N_4 Kerr OPO by modulating the pump power at fast timescales, allowing us to decouple the effects of pump power and detuning arising from thermal nonlinear resonance shifts. Our results could have implications for enhanced chip-scale sensors due to the sharp transitions near the critical point, and are useful for understanding nonlinear dynamics such as bistability and nondeterministic switching behaviors of $\chi^{(3)}$ OPOs distinct from $\chi^{(2)}$ counterparts.

- 1. Y. Zhao, Y. Okawachi, J. K. Jang, X. Ji, M. Lipson, and A. L. Gaeta, Phys. Rev. Lett. 124, 193601 (2020).
- 2. A. Marandi, Z. Wang, K. Takata, R. L. Byer, and Y. Yamamoto, Nat. Photonics 8, 937 (2014).
- 3. A. Pasquazi, et al., Phys. Rep. 729, 1 (2018).
- 4. J. R. Stone, X. Lu, G. Moille, D. Westly, T. Rahman, and K. Srinivasan, Nat. Photonics doi:10.1038/s41566 (2023).
- 5. J. A. Black, G. Brodnik, H. Liu, S.-P. Yu, D. R. Carlson, J. Zang, T. C. Briles, and S. B. Papp, Optica 9, 1183 (2022).
- 6. C. Ning, P. Liu, Y. Qin, and Z. Zhang, Opt. Lett. 45, 2551 (2020).
- 7. G. Moille, M. Leonhardt, D. Paligora, N. Englebert, F. Leo, J. Fatome, K. Srinivasan, and M. Erkintalo, arXiv:2306.04078 (2023).
- 8. Y. Okawachi, M. Yu, K. Luke, D. O. Carvalho, S. Ramelow, A. Farsi, M. Lipson, and A. L. Gaeta, Opt. Lett. 40, 5267 (2015).
- 9. A. Roy, S. Jahani, C. Langrock, M. Fejer, and A. Marandi, Nat. Commun. 12, 835 (2021).
- 10. M. He and K. Jamshidi, Phys. Rev. Appl. 20, 054036 (2023).
- 11. X. Yi, Q.-F. Yang, K. Youl, and K. Vahala, Opt. Lett. 41, 2037 (2016).
- 12. V. Brasch, M. Geiselmann, M. H. P. Pfeiffer, and T. J. Kippenberg, Opt. Express 24, 29312 (2016).